Probing Excited-State Electron Transfer by Resonance Stark Spectroscopy. 1. Experimental Results for Photosynthetic Reaction Centers

**Huilin Zhou and Steven G. Boxer***

Department of Chemistry, Stanford University, Stanford, California 94305-5080

Received: April 28, 1998; In Final Form: August 28, 1998

Higher order Stark spectroscopy has recently been introduced and applied to characterize the electrooptic properties of chromophores in bacterial photosynthetic reaction centers.[1] In the course of these studies, an unusually large and broad higher order Stark effect with a novel line shape was discovered in the region of the monomeric bacteriochlorophyll absorption band. The origin of this new feature has been explored by comparing results from reaction centers in which the chromophores are modified or the environment around the chromophores has an altered amino acid residue composition. Taken together, these results demonstrate that this unusual higher order Stark effect is related to both the monomeric bacteriochlorophyll and bacteriopheophytin on the electron-transfer pathway of the reaction center. The effects of mutations and the oxidation of the special pair on this signal specifically suggest the involvement of charge-separated species between these monomeric chromophores. In part 2 (following paper in this issue) we develop a general treatment of this phenomenon based on a charge resonance interaction between a strongly allowed transition and a charge-separated state. This leads to a variety of predicted higher order Stark line shapes which span the range observed in part 1 and from which we can obtain information on these potentially important, but heretofore experimentally inaccessible, charge-separated states.

There has been extensive experimental and theoretical work directed toward a deeper understanding of the mechanism of the initial electron-transfer steps in photosynthesis. A schematic diagram of the chromophore arrangement derived from the X-ray structure[2,3] is shown in Figure 1. Two closely interacting bacteriochlorophylls (BChls) form the dimeric special pair P, which is the primary electron donor. There are two accessory BChls designated B, two bacteriopheophytins (BPhe) designated H, and two quinones (not shown). Despite the structural pseudo C_2 symmetry obvious from the structure, electron transfer occurs predominantly along the L-branch of monomeric chromophores, as illustrated with a quantum yield approaching unity.[4−6] This extremely efficient and unidirectional electron transfer has stimulated much experimental and theoretical interest.[7−10] The role of the accessory BChl on the functional side (B_L) in facilitating the electron-transfer reaction from ^1P to $P^+H_L^-$ is an unresolved problem. Two limiting mechanisms have emerged: a two-step mechanism in which electron transfer occurs sequentially from ^1P to form the intermediate state $P^+B_L^-$ and subsequently $P^+H_L^{-}$ [11,12] and a direct one-step electron transfer from ^1P to form $P^+H_L^-$, where the $P^+B_L^-$ state serves as a virtual intermediate to enhance the electronic coupling between ^1P and $P^+H_L^-$ by superexchange.[10,13,14] In either case, the B_L molecule plays a crucial role, whether as $P^+B_L^-$ or $B_L^+H_L^{-}$.[15,16] The role of B_L no doubt is also critical to understanding the origin of unidirectional electron transfer.

All information on the energetics of these charge-transfer states in situ has been obtained by indirect methods.[17] It would be most desirable to directly observe these intermediate charge-separated states by spectroscopy from the ground state, but no data have been reported due to their small oscillator strength. On the other hand, the Q_y electronic transitions of the chromophores are likely to be energetically close to these functionally important charge-transfer states. Charge resonance inter-
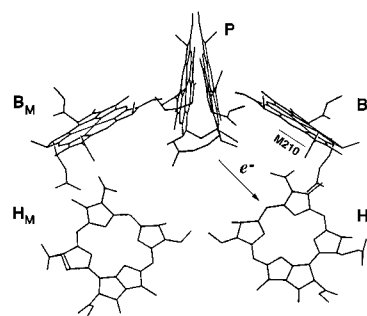
Figure 1. Schematic arrangement of the chromophores in the *Rb. sphaeroides* reaction centers derived from the X-ray structure.[33] P is the special pair BChl dimer; B and H are monomeric BChl and BPhe, respectively. Electron transfer occurs essentially exclusively along the L side. The residue at position M210 is tyrosine in wild-type and leucine in *Chloroflexus aurantiacus*. B_M is a BPhe in *C. aurantiacus*, and H_L is a BChl in the (M)L214H β mutant.

action between these first excited states and intermolecular charge-transfer states is directly responsible for the intermolecular charge-transfer process; conversely the presence of this interaction should modify the physical nature of the first excited states of chromophores. Some evidence for a large charge resonance interaction between locally excited and internal charge-transfer states of the special pair has been inferred from conventional Stark spectroscopy[18−20] and by a recent analysis of the absorption spectrum of several *Rhodobacter sphaeroides* (*Rb. sphaeroides*) heterodimer mutant reaction centers (RCs).[21] The charge resonance interactions between the accessory BChls and BPhes (e.g. B_L and H_L or B_M and H_M, each pair also a "heterodimer") in photosynthetic RCs should be weaker because the distance between them is greater. This is evident from their absorption spectra, which are qualitatively similar to those of isolated BChl and BPhe molecules, respectively,[1,18,21] and

inhomogeneous broadening obscures any information in the absorption spectrum.

We have extended conventional Stark spectroscopy with a new method called higher order Stark spectroscopy (HOSS) which measures the higher harmonic responses of the absorption to an AC electric field.[1] In the course of applying this method to photosynthetic RCs, we discovered an unusually large higher order Stark effect with an unexpected and unprecedented line shape in the region around 800 nm where the B chromophores absorb. In the following we investigate the characteristics of this new signal in several RC variants and show that it is related to some functionally important intermolecular charge-transfer states. In part 2 (the following paper in this issue), we develop a general theory for this effect and use this to obtain quantitative information on these states.

Experimental Methods

The experimental setup and sample preparation are described in detail elsewhere.[22,23] Site specific mutant *Rb. sphaeroides* strains (M)Y210F and (M)L214H (the β mutant) were generously provided by Dr. C. Schenck. Wild-type (WT) and mutant *Rb. sphaeroides* were grown semiaerobically; RCs were isolated by conventional methods and contain a single quinone, Q_A. *Chloroflexus aurantiacus* (*C. aurantiacus*) RCs were a kind gift from Dr. A. R. Holzwarth. RC samples were in 0.1% lauroyl dimethylamine oxide (LDAO), 10 mM Tris buffer (pH 8.0) unless noted otherwise. The samples for low-temperature Stark measurements were mixed with glycerol to a final composition of 50% (v/v). The $n\omega$ (where $n = 2, 4$, or 6) Stark spectra were detected using a lock-in amplifier at the nth harmonic of the applied field frequency ω. Typically the peak value of applied AC sinusoidal electric field was $0.8-1.0$ MV/cm; however, to facilitate comparison, all Stark spectra were scaled to an applied field of 1 MV/cm in the figures using the F^n-dependence of the Stark signal following demonstration that the 2ω, 4ω, and 6ω Stark spectra scale as the second, fourth, and sixth powers of the applied field, respectively. The absorption spectra were scaled such that the B band absorbance is unity except for that of *C. aurantiacus* RCs, which was scaled such that its P band had the same absorbance as that of WT *Rb. sphaeroides* RCs.

Conventional Analysis of Higher Order Stark Effect

The new results described in the following do *not* conform to expectations from the conventional treatment introduced by Liptay[24] even when extended to include the higher order Stark effect.[1] Nonetheless, this conventional treatment provides a framework for analyzing Stark data and the basis for the conclusion that what is observed cannot be explained by this conventional model; a nonconventional treatment that can explain the novel signals is presented in part 2.

The extinction coefficient $\epsilon_2(\nu)$ can be expressed as

$$\epsilon_2(\nu) = \kappa\nu|(\hat{e}\cdot\vec{m})|^2 S(\nu) \qquad (1)$$

where κ is a constant, ν is the photon energy in wavenumbers, $\hat{e}$ is the unit vector for the polarization of the probe light, $\vec{m}$ is the transition dipole moment, and $S(\nu)$ is the absorption line shape function. It is assumed that $S(\nu)$ does not itself change with applied electric field **F**, and only the transition energy is modified in an applied field. Because the electric field-induced change in absorption is usually a small perturbation to the absorption spectrum, the line shape function in an applied electric field is given as

$$S(\nu, F) = S(\nu, 0) - \frac{\partial S}{\partial \nu}\Delta\nu + \frac{1}{2}\frac{\partial^2 S}{\partial \nu^2}\Delta\nu^2 - \frac{1}{6}\frac{\partial^3 S}{\partial \nu^3}\Delta\nu^3 + ... \qquad (2)$$

where $\Delta\nu$ is the transition energy shift caused by the electric field given by

$$\Delta\nu = \frac{1}{hc}\left(\Delta\vec{\mu}_0\cdot\vec{F} + \frac{1}{2}\vec{F}\cdot\Delta\alpha\cdot\vec{F} + ...\right) \qquad (3)$$

where c is the speed of light, h is Plank's constant, $\Delta\vec{\mu}_0$ is the difference dipole moment between the ground and excited states, and $\Delta\hat{\alpha}$ is the difference polarizability tensor between the ground and excited states. The field effect on the transition dipole moment is neglected for simplicity. Substituting eqs 2 and 3 into eq 1, the electroabsorption (Stark) effect is given by

$$\Delta\epsilon_2(\nu) = \Delta\epsilon_2(\nu, F^2) + \Delta\epsilon_2(\nu, F^4) + \Delta\epsilon_2(\nu, F^6) + ... \qquad (4)$$

where odd power field-dependent changes in absorption vanish for an immobilized isotropic sample. If $\Delta\vec{\mu}_0$ makes the dominant contribution to the Stark effect, we can make the further simplification of ignoring all the polarizability tensors. The explicit forms of various field-dependent Stark effects in eq 4 can be expressed in terms of the observed change in absorbance:

$$\Delta A(n\omega,\nu) = \frac{1}{n!}\frac{\nu}{h^n c^n}\frac{\partial^n(A/\nu)}{\partial\nu^n}(f\Delta\mu_0 F)^n\, C_A^{\,n\omega}, \quad n = 2, 4, 6, ...$$
$$\Delta\vec{\mu}_0 \text{ dominates} \quad (5)$$

where f is the local field correction.[18] The angle factor $C_A^{\,n\omega}$ is a result of orientation averaging for an isotropic sample and is given as

$$C_A^{\,n\omega} = \frac{1}{(n+1)(n+3)}\Big[(n+3) + \frac{n}{2}(3\cos^2\chi - 1)(3\cos^2\zeta_A - 1)\Big] \quad (6)$$

where ζ_A is the internal angle between $\Delta\vec{\mu}_0$ and the transition dipole moment $\vec{m}$ in the molecular frame, and χ is the experimental angle between the applied field direction and the direction of polarization of the probe light.

As seen in eq 5, when $\Delta\mu_0$ dominates, the 2ω Stark spectrum has a line shape given by the second derivative of the absorption; that is, the absorption band is broadened by the applied field. The 4ω Stark spectrum has a line shape which is the fourth derivative of the absorption spectrum, and the 6ω Stark spectrum shows a sixth derivative line shape. In each case the amplitude of the Stark spectrum contains the identical information about $\Delta\mu_0$ and ζ_A. It is often difficult to determine whether the 2ω Stark spectrum is really dominated by $\Delta\mu_0$ because the experimentally determined second derivative of the absorption spectrum tends to be quite noisy. However, higher order Stark spectroscopy provides a simple test for the dominance of $\Delta\mu_0$, as seen in eq 5: the $n\omega$ Stark spectrum should have the second derivative line shape of the $(n-2)\omega$ Stark spectrum, and their *ratio* depends only on $\Delta\mu_0$ and ζ_A. We will exploit this in an inverse form in the analysis that follows: if $\Delta\mu_0$ and ζ_A can be accurately determined from the conventional 2ω Stark spectrum or reasonably inferred from the measured properties of the isolated chromophores, then the expected 4ω Stark spectrum can be calculated by taking the second derivative of the 2ω Stark spectrum and multiplying by a factor that only depends

Stark Spectroscopy Photosynthesis

J. Phys. Chem. B, Vol. 102, No. 45, 1998 **9141**
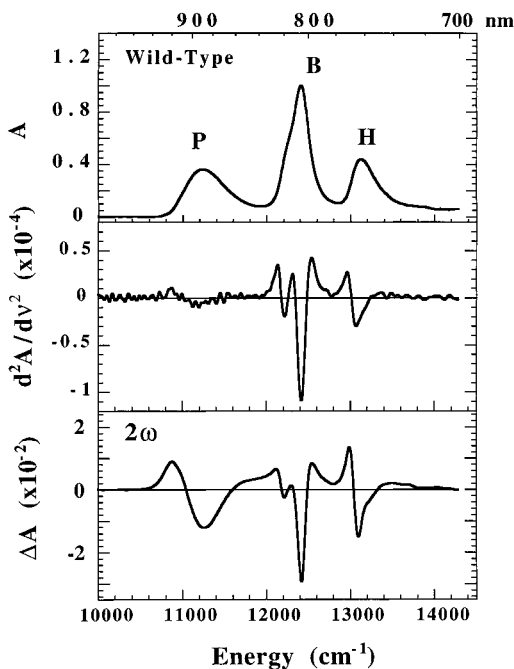
Figure 2. Absorption (top panel), second derivative of absorption (middle panel) and 2ω Stark spectrum (bottom panel) of wild-type *Rb. sphaeroides* RCs in glycerol/buffer glass at 77 K ($\chi = 90°$). The 2ω Stark spectrum was scaled to an applied field strength of 1 MV/cm in this figure and all subsequent figures to facilitate comparison.

on $\Delta\mu_0$ and ζ_A. Likewise, the 6ω Stark spectrum can be constructed from the second derivative of the 4ω Stark spectrum, and so on. Note that the local field correction term f only affects the value of $\Delta\mu_0$, not $f\Delta\mu_0$ that is used in such an analysis, and it will therefore be ignored in the following.

If the contribution from polarizability tensors such as $\Delta\hat{\alpha}$ dominates the Stark spectrum and the contribution from $\Delta\mu$ can be neglected, then, following a similar procedure as that used in deriving eq 5, the higher order Stark effects are given by

$$\Delta A(n\omega,\nu) \propto \frac{\nu}{h^n c^n} \frac{\partial^k (A/\nu)}{\partial \nu^k} (f\Delta\hat{\alpha}:F^2)^k, \quad n = 2k = 2, 4, 6, ...$$

$$\Delta\hat{\alpha} \text{ dominates} \quad (7)$$

where the sample average has not been performed as this only introduces a proportionality constant. In this case, the 2ω Stark spectrum line shape will be given by the first derivative of the absorption, that is, a band-shift line shape whose sign depends on the sign of $\Delta\hat{\alpha}$. The 4ω Stark spectrum will have a *positive* second derivative line shape of the absorption, and the 6ω Stark spectrum will have a third derivative line shape of the absorption spectrum with the same sign as the 2ω Stark spectrum. Thus, even when $\Delta\hat{\alpha}$ makes the dominant contribution, one expects that the higher order Stark spectra should have higher order derivative line shapes. As seen in the following, the new higher order Stark signals observed in photosynthetic RCs do not have these higher order derivative line shapes and therefore cannot be understood in terms of the conventional model.

Results

Wild-Type *Rb. sphaeroides* RCs. The absorption, the second derivative of the absorption, and the conventional 2ω Stark spectrum for WT *Rb. sphaeroides* RCs are shown in Figure 2. The 2ω Stark spectra for both the B and H bands have the second derivative line shapes of their absorption bands, which suggests that $\Delta\mu_0$ dominates the 2ω Stark spectra.[9] ΔA
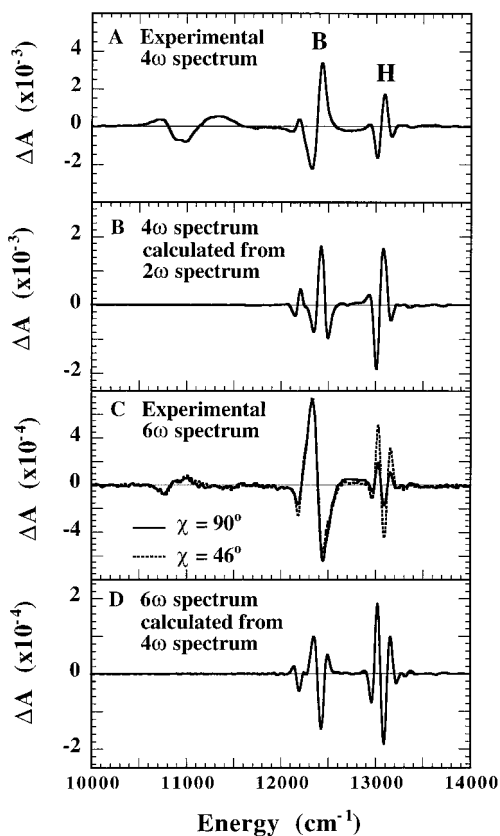

Figure 3. (A) Experimental 4ω Stark effect spectrum; (B) calculated 4ω Stark effect spectrum derived from the second derivative of the 2ω spectrum (lower panel Figure 3); (C) experimental 6ω Stark effect spectrum at two different experimental angles, $\chi = 90°$ (—) and $\chi = 46°$ (--); (D) calculated 6ω Stark effect spectrum derived from the second derivative of the 4ω spectrum shown in panel (A) for wild-type *Rb. sphaeroides* RCs (same sample as Figure 3, 77 K, $\chi = 90°$).

for the H band was measured as a function of χ, giving $\zeta_A = 30 \pm 2°$, and, using eq 5, $\Delta\mu_0$ is found to be 3.5 $\pm$ 0.5 D/f. The band around 760 nm is composed of two overlapping BPhe monomer Q_y transitions, with the BPhe on the L side (H_L) narrower and therefore dominating the Stark effect spectrum. A more elaborate analysis shows that the H_M and H_L transitions have approximately the same $\Delta\mu_0$ and ζ_A.[9]

In the B band region around 800 nm, there are two negative peaks in the second derivative and 2ω Stark spectra, one at 810 nm and the other at 800 nm. On the basis of eq 5, $\Delta\mu_0$ for the 800 nm is 2.9 $\pm$ 0.2 D/f and ζ_A is 38 $\pm$ 2°, while $\Delta\mu_0$ for the 810 nm band is 2.3 $\pm$ 0.2 D/f and ζ_A is 30 $\pm$ 2°. The Stark effect of the 800 nm band appears to have a smaller dependence on the experimental angle χ than the 810 nm or the H bands because its ζ_A is closer to the magic angle (see eq 6). The difference dipole moments and line widths of these two B bands are similar to those of isolated monomeric BChl in an organic glass.[1,18] Most of the oscillator strength in this region comes from the two accessory BChl transitions, though some oscillator strength may derive from the upper exciton band of P.[11,25]

Given that $\Delta\mu_0$ appears to dominate the 2ω Stark effects of both the B and H bands, we expect a fourth derivative line shape for the 4ω Stark spectrum and a sixth derivative line shape for the 6ω Stark spectrum, as seen in eq 5. The experimental 4ω Stark spectrum ($\chi = 90°$) is shown in Figure 3A. The experimental 6ω Stark spectra at two different experimental angles, $\chi = 90°$ and $46°$, are shown in Figure 3C. The higher order Stark spectra in the B band region appear to be broader and increasingly more dominant compared with the H bands.
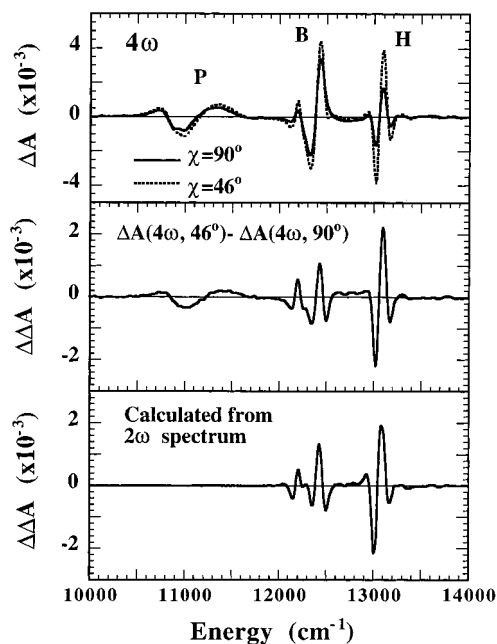
Figure 4. (A, top) Experimental 4ω Stark spectra for wild-type *Rb. sphaeroides* at two different experimental angles, $\chi = 90°$ (—) and $\chi = 46°$ (--); (B, middle) the difference 4ω Stark spectrum between the two spectra in A; and (C, bottom) the calculated difference spectrum derived from the 4ω Stark spectra at the same two experimental angles.

If $\Delta\mu_0$ makes the dominant contribution to the Stark effects, we can calculate the expected 4ω Stark spectrum from the second derivative of the 2ω Stark spectrum and the expected 6ω Stark spectrum from the second derivative of the 4ω Stark spectrum. The calculated 4ω and 6ω Stark spectra ($\chi = 90°$ for both) are shown in Figure 3B,D, respectively.[26] There is good agreement for both the line shapes and amplitudes between the experimental higher order Stark spectra and the calculated spectra for the H bands; however, the agreement in the B band region is poor as a broad feature is present. The conventional analysis of the 2ω Stark spectrum demonstrates that the values of ζ_A for the H and B bands are similar,[9,18] and this similarity should be preserved in the higher order spectra if $\Delta\mu_0$ dominates (see eq 6). Interestingly, we notice that both the amplitude and line shape of the broad 6ω Stark effect hardly depend on the experimental angle χ, while the amplitude of the 6ω Stark spectra of the H band depends strongly on the experimental angle χ, as expected from the value of ζ_A for the H band and eq 6. This can be further exploited in the following.

Figure 4A shows the 4ω Stark spectra for the same two experimental angles as in Figure 3C. Small differences are observed in the B band region, but a large *amplitude* difference is found in the H band region. Figure 4B shows the *difference* between the 4ω Stark spectra obtained at these two values of χ. This can be compared with the expected difference in the 4ω Stark spectra shown in Figure 4C obtained by subtracting the second derivatives of the experimental 2ω Stark spectra obtained at $\chi = 90$ and $46°$. Significantly, both the line shapes and amplitudes in *both* the B and H band regions in Figure 4B,C are quite similar, which suggests that the Stark effect due to the $\Delta\mu_0$ of the BChls in the 800 nm region is still present, even though a broader and much more intense feature with little χ dependence increasingly dominates the higher order spectra. By subtracting the expected (due to $\Delta\mu_0$ only) higher order Stark spectra (Figure 3B,D) from the experimental spectra in Figure 3A,C, we uncover the unusually broad higher order Stark line shapes in the B band region (Figure 5). The 6ω difference Stark
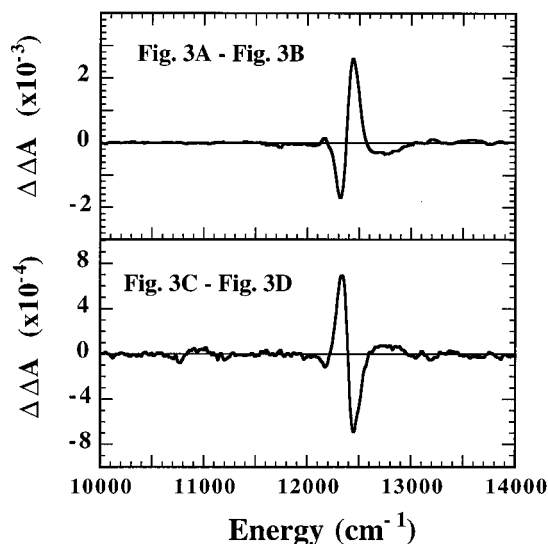

Figure 5. (A, top) Difference between the Stark spectra in Figure 3A,B and (B, bottom) difference between spectra in Figure 3C,D. This subtraction is intended to obtain the line shapes of the unusual Stark effect of B band.

spectrum in Figure 5B has neither a first or second derivative line shape of the 4ω difference Stark spectrum in Figure 5A; instead, its line shape appears more like the inverted 4ω Stark spectrum. As discussed above, neither $\Delta\mu_0$ or $\Delta\hat{\alpha}$ or a combination of these contributions can account for this behavior, so a different mechanism is necessary. In the following we exploit this simple subtraction method; the underlying validity of this approach is discussed in part 2.

Oxidized P in Wild-Type *Rb. sphaeroides* RCs. To determine whether some underlying higher energy transition of P is responsible for the broad higher order Stark effect feature in the B band region, we oxidized P to form P^+ by adding 300 mM potassium ferricyanide. The absorption, the second derivative of the absorption, and 2ω Stark spectra are shown in Figure 6. The P band and its Stark effect in the 800−900 nm region are almost completely lost, as expected, because P^+ absorbs only weakly in this region. The H band absorption and Stark effect spectra are shifted to lower energy compared to RCs with neutral P (compare Figure 2) due to electrochromic band shifts which have been analyzed in detail elsewhere.[9] The 2ω Stark spectrum of the H band (now poorly resolved as the electrochromic shift for H_M is greater than for H_L[9]) shows a second derivative line shape of its absorption spectrum; quantitative analysis gives $\Delta\mu_0 = 3.5 \pm 0.5$ D/f and $\zeta_A = 18 \pm 2°$. Detailed line shape analysis shows that the 2ω Stark spectra for the B bands have contributions from both a second derivative and a *positive* first derivative line shape. The second derivative contribution allows $\Delta\mu_0$ to be obtained (the spectral separation for B_M and B_L is substantially smaller in P^+ RCs than in the neutral as the lower energy B_M band shifts more to higher energy than B_L[9]). Quantitative analysis shows $\Delta\mu_0 = 2.7 \pm 0.3$ D/f and $\zeta_A = 35 \pm 3°$, comparable to neutral RCs and to isolated BChl.[1] The *positive* first derivative feature in the 2ω Stark effect on the B band is unexpected since this was not found in the 2ω Stark effect spectrum of isolated BChl.[1]

The 4ω and 6ω higher order Stark spectra of P^+-containing RCs are shown in Figure 7A,C, respectively. As in the analysis of neutral RCs (see Figure 2), we calculate the expected 4ω Stark spectrum from the second derivative of the 2ω Stark spectrum and the expected 6ω Stark spectrum from the second derivative of 4ω Stark spectrum,[26] and these are shown in Figure 7B,D, respectively. As for neutral RCs, the 4ω and 6ω Stark

Stark Spectroscopy Photosynthesis

*J. Phys. Chem. B, Vol. 102, No. 45, 1998* **9143**
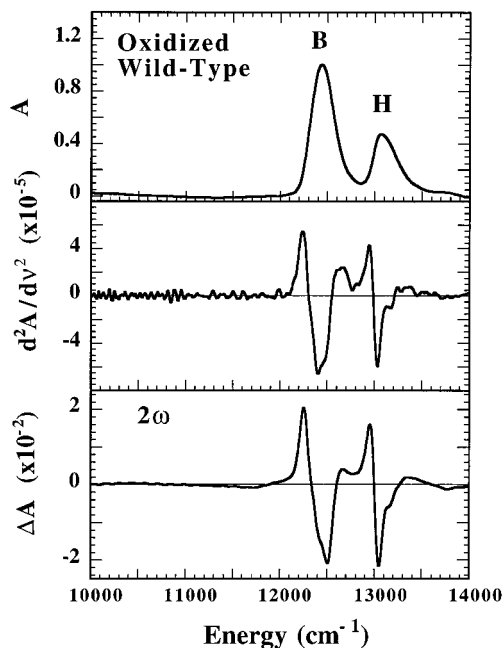
Figure 6. Absorption (top panel), second derivative of absorption (middle panel), and 2ω Stark spectrum (bottom panel) of wild-type *Rb. sphaeroides* RCs in which P has been oxidized to P^+ by addition of ferricyanide (glycerol/buffer glass at 77 K, $\chi = 90°$).
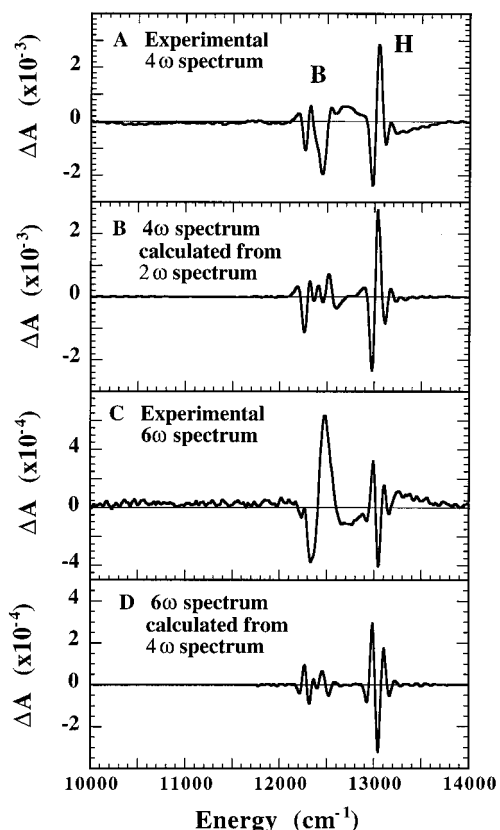
Figure 7. (A) Experimental 4ω Stark effect spectrum; (B) calculated 4ω Stark effect spectrum derived from the second derivative of the 2ω spectrum (lower panel Figure 6); (C) experimental 6ω Stark effect spectrum; and (D) calculated 6ω Stark effect spectrum derived from the second derivative of the 4ω spectrum shown in panel A for oxidized wild-type *Rb. sphaeroides* RCs (same sample as Figure 6, 77 K, $\chi = 90°$).

spectra in the H band region agree very well with the calculated Stark spectra, as expected when 1 dominates the Stark effect. By contrast, in the B band region a broader higher order Stark
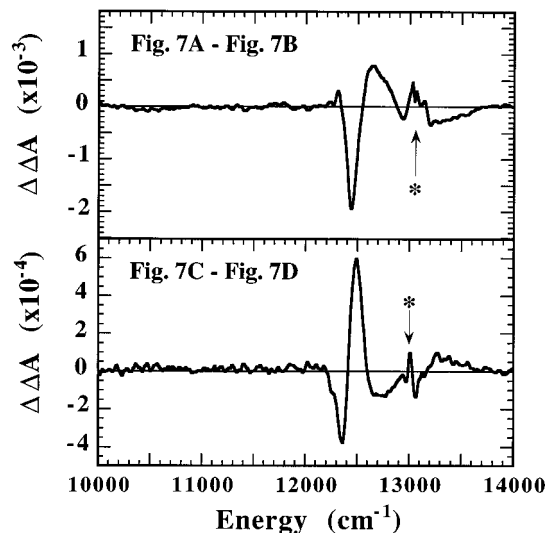

Figure 8. (A, top) Difference between the Stark spectra in Figure 7A,B and (B, bottom) difference between spectra in Figure 7C,D. The asterisk around 13 000 cm^{-1} indicates where the higher order Stark spectra of the H bands are not perfectly subtracted.

spectrum is seen, which completely dominates the 6ω spectrum. The calculated higher order Stark spectra for the B band (Figure 7B,D) are similar to the higher order derivative line shapes of the bands seen in neutral RCs (compare Figure 3B,D), except that the positions of the bands are electrochromically shifted to higher energy. Because of the much better signal-to-noise ratio, it is easier to obtain the higher order derivative line shapes of overlapping bands such as in the B region, than from the absorption spectra. Examination of the expected derivative spectra suggests that the two bands in P^+ RCs are likely due to the accessory B_L and B_M transitions. Furthermore, because the upper exciton transition of P is absent when P is oxidized to P^+, the upper exciton transition of P is clearly not responsible for the unusually large higher order Stark effects in the B band region.

As for neutral wild-type RCs (Figure 3C), the broad 6ω Stark feature in the B band region for P^+-containing RCs also has little dependence on experimental angle χ (data not shown). Thus, the same strategy was used to extract the pure line shape of this unusual higher order Stark spectrum, and this is shown in Figure 8. The sharp features around 13 000 cm^{-1} are due to imperfection in subtracting the H band Stark effects. Comparing this result for P^+-containing RCs with the spectra in Figure 5 for neutral RCs, we find interesting similarities and differences. Both are broader than the higher order Stark spectra of monomeric BChl or BPhe due to the usual dipole mechanism, become more dominant in the higher order Stark spectra, and have much smaller χ dependencies than for the monomeric BChl and BPhe transitions, and in both cases the 6ω spectrum is approximately an "inverted" 4ω spectrum. We thus suggest that the broad higher order Stark spectra shown in Figures 5 and 8 have the same origin and apparently are not associated with electronic transitions of the special pair, as any feature in this region would disappear when P is oxidized. Significantly, however, the line shape and amplitude of this feature do depend on the net charge on P.

β Mutant. The absorption and higher order Stark spectra for the β mutant [(M)H214L], in which a BChl molecule absorbing at 785 nm replaces the BPhe molecule in the H_L binding site,[27] are shown in the left column of Figure 9. The 2ω Stark spectrum for the B, β_L, and H_M bands has the second derivative line shape of the absorption spectrum. Conventional
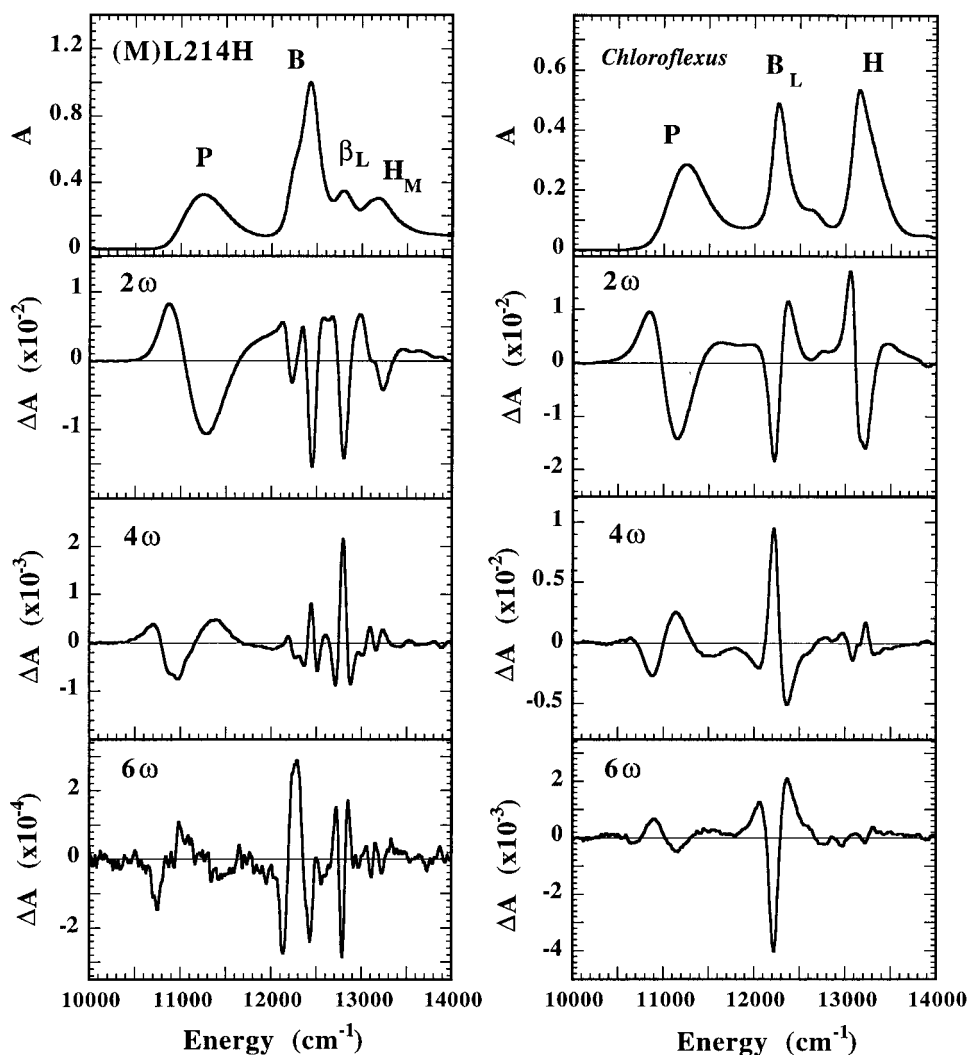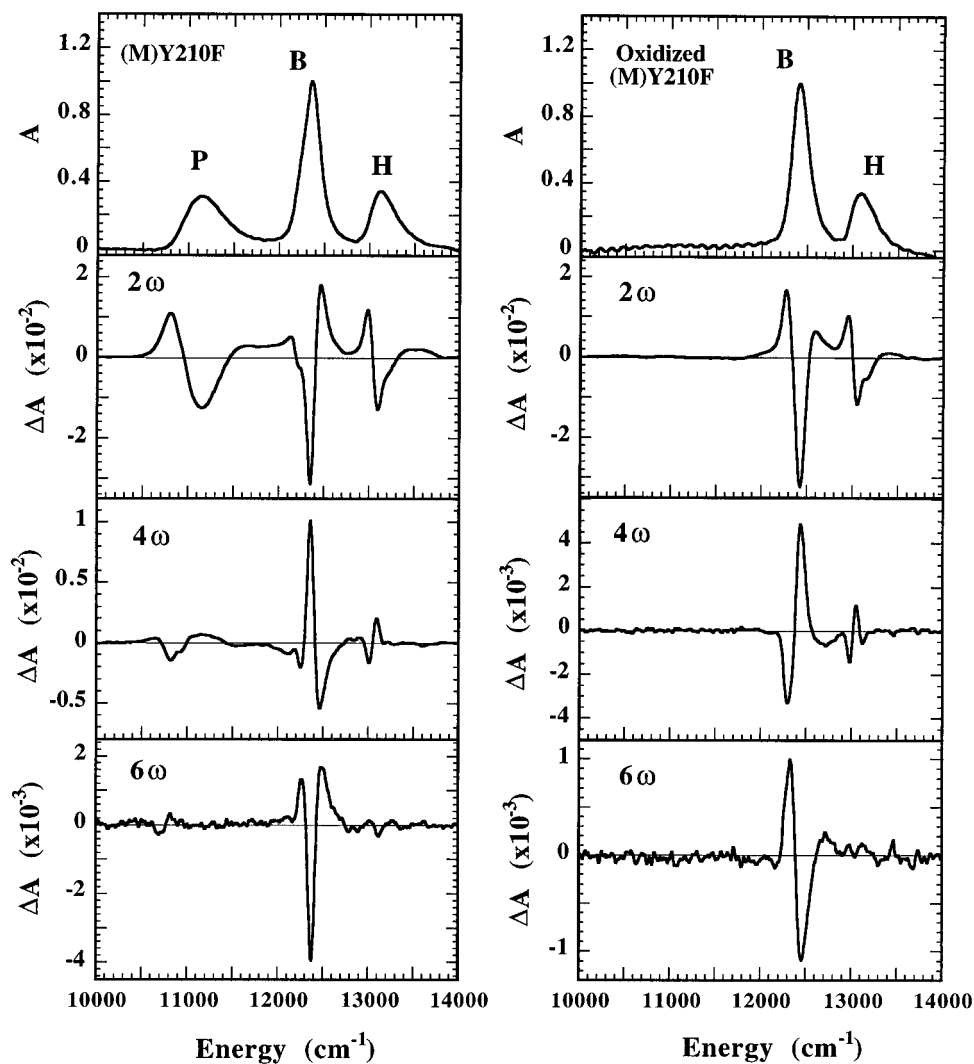
Figure 9. Left column: absorption, 2ω, 4ω, and 6ω Stark spectra of the (M)L214H mutant RCs (the β-mutant) of *Rb. sphaeroides* (77 K, $\chi = 90°$). Right column: absorption, 2ω, 4ω, and 6ω Stark spectra of *Chloroflexus aurantiacus* RCs (77 K, $\chi = 90°$).

analysis of the β_L band gives $\Delta\mu_0 = 3.6 \pm 0.5$ D/f and $\zeta_A = 27 \pm 2°$, approximately the same values obtained for the H_M band, and nearly identical values $\Delta\mu_0 = 2.2 \pm 0.2$ D/f and $\zeta_A = 35 \pm 2°$ for both B bands. The Stark effect for the special pair is comparable to that of WT RCs (compare Figure 2). The amplitude of the 2ω Stark effect of the β_L band is comparable to that of the H_L band in WT *Rb. sphaeroides* RCs despite their rather different line shapes. The 2ω Stark effect of the B bands appears to be smaller in the β-mutant than in WT, though their second derivative spectra are nearly identical, which is the reason that the derived difference dipole moments for the B bands in the β_L-mutant are somewhat smaller. The 4ω Stark spectra for the B, β_L, and H_M bands all have the second derivative line shape of their corresponding 2ω Stark spectra, which suggests that $\Delta\mu_0$ is mainly responsible for both 2ω and 4ω Stark effects of these bands; quantitative analysis based on a comparison of the 4ω Stark spectrum and the second derivative of the 2ω Stark spectrum agrees with the results given above by conventional analysis of the 2ω Stark spectrum. The 4ω Stark spectrum in the B band region of the β-mutant is very different from that in WT *Rb. sphaeroides* RCs (compare with Figure 3A). Interestingly it has a line shape that is very similar to the calculated, not observed, 4ω Stark spectrum of the B region of WT (Figure 3B); i.e., the broader feature that dominates for WT is nearly absent in the 4ω Stark spectrum of the β-mutant. The 6ω Stark spectrum of the β_L band in Figure 9 has the second derivative

line shape of the corresponding 4ω Stark spectrum as expected. A broader feature is now observed in the B band region of the 6ω Stark spectrum; however, this broad 6ω Stark effect is much smaller in amplitude than the broad 6ω Stark effects in WT or P-oxidized WT shown in Figures 5 and 8, respectively. This suggests that the new feature in the B band region depends strongly on the chromophore in the H_L binding site.

Chloroflexus aurantiacus **RCs.** *C. aurantiacus* RCs were examined because there is a BPhe molecule instead of a BChl molecule in the B_M binding site.[28] The absorption and higher order Stark spectra are shown in the right column of Figure 9. The H band region now consists of three unresolved BPhe transitions, and a quantitative analysis was not attempted. Nevertheless the amplitudes of the higher order Stark effects are comparable to those for the H bands of WT *Rb. sphaeroides* RCs. The 2ω Stark spectrum of the B_L band at 12 220 cm^{-1} shows mostly a *negative* first derivative line shape of absorption, suggesting a band-shift mechanism. This feature is absent in isolated BChl[1] and is qualitatively different from the previous examples in Figures 2, 6, and the left column of Figure 9. The 4ω Stark spectrum has mostly a band-*narrowing* line shape, i.e., increased absorbance at the peak and decreased absorbance at either wings of the absorption. The 6ω Stark spectrum shows mostly a band-*broadening* line shape, similar to an "inverted" 4ω Stark line shape. Despite the large differences in line shapes and amplitudes, the broad higher order Stark spectra shown in

Stark Spectroscopy Photosynthesis

J. Phys. Chem. B, Vol. 102, No. 45, 1998 **9145**

Figure 10. Left column: absorption, 2ω, 4ω, and 6ω Stark spectra of the (M)Y210F mutant RCs of *Rb. sphaeroides* (77 K, $\chi = 90°$). Right column: absorption, 2ω, 4ω, and 6ω Stark spectra of the (M)Y210F mutant of *Rb. sphaeroides* RCs oxidized with ferricyanide (77 K, $\chi = 90°$). The oscillations in the baseline in the $820-1000$ nm region of the absorption spectrum are interference fringes.

the right column of Figure 9 and the higher order Stark spectra around B band in Figures 5 and 8 share some characteristics. They are much larger and broader than the higher order Stark spectra of the H band and exhibit weak χ dependence. Interestingly, the 6ω Stark spectrum line shape appears to resemble the inverted 4ω Stark spectrum line shape in both cases.

(M)Y210F Mutant. The higher order Stark spectra for the *Rb. sphaeroides* (M)Y210F mutant are shown in the left column of Figure 10. A comparison with the data for wild-type *Rb. sphaeroides* (Figures 2 and 3) and *C. aurantiacus* (right column of Figure 9) is revealing. There is little difference in the higher order Stark effects for the P and H bands between wild-type and the (M)Y210F mutant; however, there are striking differences in the B band region. Significantly, the higher order Stark spectra in the B band region of the *Rb. sphaeroides* (M)Y210F mutant are very similar to those of *C. aurantiacus*; the latter RCs have a leucine at position M210 instead of a tyrosine.

Oxidized Special Pair in the (M)Y210F Mutant. The special pair in the *Rb. sphaeroides* (M)Y210F mutant was oxidized with 300 mM potassium ferricyanide, and the higher order Stark spectra are shown in the right column of Figure 10. The line shape of the 2ω Stark spectrum in the B band region shows mostly a second derivative of absorption line shape with an amplitude comparable to that for the wild-type (Figure 2).

Surprisingly, both the amplitude and line shape of the higher order 4ω and 6ω Stark spectra in the B band region are very similar to those for *unoxidized* wild-type *Rb. sphaeroides* (Figure 5). As in all other cases, we also found little dependence of the higher order Stark effects in the B band region on the experimental angle χ (data not shown). Clearly the special pair P is not directly involved in producing the unusual higher order Stark effects in the B band region, but the charge on P^+ does change the line shape. This result further suggests that the higher order Stark effects of the B band in neutral (M)Y210F mutant (or in *C. aurantiacus* RCs) should share the same origin as those for WT *Rb. sphaeroides* RCs. The BChl molecule in the B_M binding site should have nothing to do with these unusual Stark spectra in the B band region as it is absent in the *C. aurantiacus* RCs.

Discussion

Summary and Classification of Results. Three classes of unusual higher order Stark effect line shapes were observed in the B band region.

Type I Stark Line Shape. We denote the broad higher order Stark effect observed in the unoxidized (M)Y210F mutant of *Rb. sphaeroides* RCs (Figure 10, *left*) and *C. aurantiacus* RCs (Figures 9, *right*) a type I Stark effect. The peaks of the 2ω and 4ω Stark effects change signs, as do the 4ω and 6ω Stark

spectra; their line shapes are rather similar, with the 4ω and 6ω Stark spectra more similar than the 2ω and 4ω Stark spectra. Qualitatively, the evolution of the line shape can be described as follows: the 2ω Stark spectrum has largely a negative first derivative line shape, i.e., band *shift* to higher energy, the 4ω Stark spectrum has less contribution from a band-shift line shape (centro-asymmetric) and more contribution from a band-*narrowing* line shape (centrosymmetric), and this trend continues in the 6ω Stark spectrum, which has mostly a band-broadening line shape with little band-shift line shape contribution.

Type II Stark Line Shape. We denote the broad higher order Stark effect in P^+-containing (M)Y210F mutant or WT *Rb. sphaeroides* RCs a type II Stark effect (Figures 2, 5, and 10, *right*). The 2ω and 4ω Stark spectra are approximately inverted, as are the 4ω and 6ω Stark spectra; this line shape inversion is more evident between the 4ω and 6ω Stark spectra than between the 2ω and 4ω Stark spectra. The 2ω Stark effect has a mostly band-broadening line shape, most of which is likely the result of the dipole moment contribution due to the conventional mechanism.[30] The 4ω Stark spectrum has relatively more contribution from a band-*shift* and asymmetric line shape, and this trend is continued in the 6ω Stark spectrum, which has almost completely a band-*shift* line shape.

Type III Stark Line Shape. We denote the broad higher order Stark effect in P^+-containing WT *sphaeroides* RCs a type III Stark effect (Figures 6 and 8). In contrast to the type I Stark effect, the 2ω Stark spectrum has largely a *positive* first derivative line shape, i.e., band *shift* to lower energy. The 4ω Stark spectrum becomes somewhat more symmetric, while the 6ω Stark spectrum has mostly a band-*narrowing* line shape, in contrast to the 6ω Stark line shape of the type I Stark effect (band-broadening). It is interesting to note that the 4ω and 6ω Stark spectra in Figure 8 extend into the H band region. This unusual broad feature will be discussed later, and its origin is modeled in the accompanying paper (part 2).

It is evident that all three types of higher order Stark effect line shapes are very different from what is predicted from the conventional analysis described in the Experimental Methods, in contrast to line shapes in the H band region, which are well described by the conventional method. Thus, it is not possible to analyze any of these new line shapes in conventional terms to obtain $\Delta\mu_0$ and $\Delta\hat{\alpha}$. Despite the classification into three types of line shapes, they do share some common characteristics. First, compared with the corresponding higher order Stark spectra of the H band, where $\Delta\mu_0$ dominates and the conventional analysis works well, the new line shapes are broader and their amplitudes become relatively dominant (see, for example, Figure 10 where the 6ω spectrum is completely dominated by the new effect). Second, in all cases there is an approximate line shape inversion, as opposed to any derivative relationship, between $n\omega$ and $(n + 2)\omega$ Stark spectra, which is particularly evident between the 4ω and 6ω Stark spectra. Third, from a lower to a higher order Stark spectrum, there is a continuous line shape evolution from a band-broadening (or narrowing) to a band-shift line shape, or vice versa. Among all $n\omega$ Stark effects from these three types classified above, there is also such line shape evolution. Fourth, while the amplitudes of the higher order Stark spectra of the H band shows a large dependence on the experimental angle χ, the amplitudes of the new higher order Stark effects have little angle χ dependence. Last, in the 6ω Stark spectra, the broad higher order Stark effect appears to have the smallest amplitude for type III, type II an intermediate amplitude, and type I the largest amplitude. Taken together these results suggest that the

three types of broad higher order Stark effects share a common origin with differences resulting from particular aspects of each type of RC.

Physical Origin of the Novel Higher Order Stark Effect. It is revealing that the higher order Stark spectra of P^+-containing (M)Y210F mutant *Rb. sphaeroides* RCs are nearly identical to those of WT *Rb. sphaeroides* RCs (Figure 5 and right column of Figure 10). There can be no contribution to the new feature from P in the oxidized RCs. The positive charge on P^+ changes the type I Stark effect of (M)Y210F RC to the type II Stark effect, as seen in Figure 10, and it changes the type II Stark effect of WT *Rb. sphaeroides* RCs into a type III Stark effect, as seen in Figures 5 and 8. The close similarity between the new signal in *Rb. sphaeroides* (M)Y210F and *C. aurantiacus* RCs is also very informative (compare Figures 9 and 10). Both RCs have a hydrophobic residue at position (M)210, which is in close proximity to the accessory BChl (B_L) on the functional L branch (see Figure 1).[31] In contrast, there is a tyrosine residue at position (M)210 in WT *Rb. sphaeroides* RCs, and in this case the broad higher order Stark effects on the B band are very different. Therefore, they are very sensitive to the local amino acid residue environment around B_L. Furthermore, because the broad higher order Stark effects also occur on the B band in *C. aurantiacus* RCs, which only has one accessory BChl monomer (in the B_L site), one can exclude the involvement of the accessory BChl on the M branch in *Rb. sphaeroides* RCs (see ref 34, part 2). The results for the β-mutant, where a BChl replaces BPhe in the H_L binding site, suggest that the native BPhe is involved. These results further suggest that some property of B_L and H_L, not B_M and H_M, are involved in the new signal. Furthermore, because the new signal is sensitive to the charge on the special pair and to the ease of reduction of the chromophore in the H_L site, we are led to suggest that it is likely that an intermolecular CT state such as $B_L{}^+H_L{}^-$ (or $B_L{}^-H_L{}^+$) is involved. The energy of such a state is expected to be strongly perturbed when a hydrophobic residue replaces tyrosine next to B_L, as in the (M)Y210F mutant[29] or in *C. aurantiacus* RCs or in the β mutant because BChl is substantially harder to reduce than BPhe.[32]

Having identified the interaction between ^{1}B and the $B_L{}^+H_L{}^-$ (or $B_L{}^-H_L{}^+$) state as a likely candidate for the origin of the novel higher order Stark effect, it would be very desirable to obtain information on the energy of this charge-separated state and the electronic interaction between these states, from which one obtains the rate of electron transfer $^1B \rightarrow B_L{}^+H_L{}^-$ and a consistent understanding of the factors that lead to the variations among the type I−III signals. This is not possible within the framework of the conventional theory, and a new theory on Stark effects due to charge transfer is developed in detail in part 2.

References and Notes

(1) Lao, K.; Moore, L. J.; Zhou, H.; Boxer, S. G. *J. Phys. Chem.* **1995**, *99*, 496.
(2) Deisenhofer, J.; Epp, O.; Miki, K.; Huber, R.; Michel, H. *J. Mol. Biol.* **1984**, *180*, 385.
(3) Deisenhofer, J.; Epp, O.; Miki, K.; Huber, R.; Michel, H. *Nature* **1985**, *318*, 618.
(4) Kirmaier, C.; Holten, D. In *Photosynthesis Research*; Martinus Nijhoff Publishers: Dordrecht, The Netherlands, 1987; Vol. 13, pp 225−260.

Stark Spectroscopy Photosynthesis

J. Phys. Chem. B, Vol. 102, No. 45, 1998 **9147**

(5) Du, M.; Rosenthal, S. J.; Xie, X.; DiMagno, T. J.; Schmidt, M.; Hanson, D. K.; Schiffer, M.; Norris, J. R.; Fleming, G. R. *Proc. Natl. Acad. Sci. U.S.A.* **1992**, *89*, 8517−8521.

(6) Vos, M. H.; Rappaport, F.; Lambry, J.-C.; Breton, J.; Martin, J.-L. *Nature* **1993**, *363*, 320.

(7) Lockhart, D. J.; Kirmaier, C.; Holten, D.; Boxer, S. G. *J. Phys. Chem.* **1990**, *94*, 6987.

(8) Holzapfel, W.; Finkele, U.; Kaiser, W.; Oesterhelt, D.; Scheer, H.; Stilz, H. U.; Zinth, W. *Proc. Natl. Acad. Sci. U.S.A.* **1990**, *87*, 5168.

(9) Steffen, M. A.; Lao, K.; Boxer, S. G. *Science* **1994**, *264*, 810.

(10) Gehlen, J. N.; Marchi, M.; Chandler, D. *Science* **1994**, *263*, 499.

(11) Parson, W. W.; Warshel, A. *J. Am. Chem. Soc.* **1987**, *109*, 1987.

(12) Hanson, H. K.; Thompson, M. A.; Zerner, M. C.; Fajer, J. In *the photosynthetic bacterial reaction center-structure and dynamics*; Breton, J., Vermeglio, A., Eds.; Plenum Press: New York, 1988; p 355.

(13) Won, Y.; Friesner, R. A. *Biochim. Biophys. Acta* **1988**, *935*, 9.

(14) Marchi, M.; Gehlen, J. N.; Chandler, D.; Newton, M. *J. Am. Chem. Soc.* **1993**, *115*, 4178.

(15) Warshel, A.; Creighton, S.; Parson, W. W. *J. Phys. Chem.* **1988**, *92*, 2696.

(16) Scherer, P. O. J.; Fischer, S. F. *Chem. Phys. Lett.* **1987**, *141*, 179.

(17) Goldstein, R. A.; Takiff, L.; Boxer, S. G. *Biochim. Biophys. Acta* **1988**, *934*, 253.

(18) Lockhart, D. J.; Boxer, S. G. *Proc. Natl. Acad. Sci. U.S.A.* **1988**, *85*, 107.

(19) Middendorf, T. R.; Mazzola, L. T.; Lao, K.; Steffen, M. A.; Boxer, S. G. *Biochim. Biophys. Acta* **1993**, *1143*, 223.

(20) Hammes, S. L.; Mazzola, L.; Boxer, S. G.; Gaul, D. F.; Schenck, C. C. *Proc. Natl. Acad. Sci. U.S.A.* **1990**, *87*, 5682.

(21) Zhou, H.; Boxer, S. G. *J. Phys. Chem.* **1997**, *101*, 5759.

(22) Boxer, S. G. In *Biophysical Techniques in Photosynthesis*; Amesz, J., Hoff, A., Eds.; Academic: Amsterdam, The Netherlands, 1996; Vol. 3, pp 177−189.

(23) Bublitz, G. U.; Boxer, S. G. *Annu. Rev. Phys. Chem.* **1997**, *48*, 213.

(24) Liptay, W. In *Excited states*; Lim, E. C., Ed.; Academic: New York, 1974; p 120.

(25) Breton, J. *Biochim. Biophys. Acta* **1985**, *810*, 235.

(26) The expected 6ω Stark spectrum calculated from the fourth derivative of the 2ω Stark spectrum is similar, but more noisy.

(27) Kirmaier, C.; Gaul, D.; Debey, R.; Holten, D.; Schenck, C. C. *Science* **1991**, *251*, 922.

(28) Kirmaier, C.; Blankenship, R. E.; Holten, D. *Biochim. Biophys. Acta* **1986**, *850*, 275.

(29) Parson, W. W.; Chu, Z.-T.; Warshel, A. *Biochim. Biophys. Acta* **1990**, *1017*, 251.

(30) Part of the 2ω Stark effect should have the same origin as the unusual Stark effects, which are more evident in a higher order Stark spectrum. This is in fact predicted in the accompanying paper (part 2, following paper in this issue). The relative contributions from the usual Stark effect due to dipole moment (second derivative line shape, band-broadening effect) and the unusual Stark effect (band-broadening effect due to lifetime change) are difficult to separate because their line shapes are similar (also see Part 2 Appendix).

(31) The X-ray structure has not been determined, but the high level of sequence homology and similarity of RC structures from other species make it very likely that *Chloroflexus aurantiacus* RCs are structurally similar to *Rb. sphaeroides* and *Rps. viridis* RCs. See also ref 34 in part 2.

(32) Fajer, J.; Brune, D. C.; Davis, M. S.; Forman, A.; Spaulding, L. D. *Proc. Natl. Acad. Sci. U.S.A.* **1975**, *72*, 4956.

(33) Ermler, U.; Fritzsch, G.; Buchanan, S. K.; Michel, H. *Structure* **1994**, *2*, 925.